Biosensors and Bioelectronics 31 (2012) 49–54

Contents lists available at SciVerse ScienceDirect

Biosensors and Bioelectronics

journal homepage: www.elsevier.com/locate/bios

Electrochemical biosensor based on graphene oxide–Au nanoclusters composites for L-cysteine analysis

Shenguang Ge[a], Mei Yan[a], Juanjuan Lu[a], Meng Zhang[a], Feng Yu[b], Jinghua Yu[a,*], Xianrang Song[c], Shilin Yu[a]

[a] Shandong Provincial Key Laboratory of Fluorine Chemistry and Chemical Materials, School of Chemistry and Chemical Engineering, University of Jinan, Jinan 250022, China
[b] School of Mechanical and Aerospace Engineering, Nanyang Technological University, 50 Nanyang Avenue, 639798, Singapore
[c] Cancer Research Center, Shandong Tumor Hospital, Jinan 250012, China

ARTICLE INFO

Article history:
Received 27 July 2011
Received in revised form
20 September 2011
Accepted 23 September 2011
Available online 5 October 2011

Keywords:
L-Cysteine
Graphene oxide
Au nanocluster
Electrochemical biosensor

ABSTRACT

In this paper, a linker-free connected graphene oxide/Au nanocluster (GO–Au NCs) composite was prepared under sonication through electrostatic interactions, and characterized by transmission electron microscope (TEM), atomic force microscope (AFM), ultraviolet–visible (UV–vis) and FT-IR spectrum. The morphological and structural characterizations evidence that the Au NCs can be efficiently decorated on the GO. The electrochemical investigations indicated that GO–Au NCs composite has an important role in the electrocatalytic activity towards the oxidation of L-cysteine (CySH). The GO–Au NCs composite modified electrode shows a large determination range from 0.05 to 20.0 μmol/L, a remarkably low detection limit is 0.02 μmol/L and low oxidation potential (+0.387). It was found that metal ions, carbohydrates, nucleotide acids and amino acids had no distinct effect on the determination of L-cysteine. In addition, the sensor has some important advantages such as simple preparation, fast response, good stability and high reproducibility. The direct determination of free reduced and total CySH in human urine samples has been successfully carried out without the assistance of any separation techniques.

1. Introduction

L-Cysteine (CySH) plays a key role in biological systems owing to its crucial roles. It is known to be an active site in the catalytic function of certain enzymes called cysteine proteases and in many other peptides and proteins (Ardakani et al., 2007; Lai et al., 2010). Low level of CySH is associated with a number of clinical situations, such as slowed growth, hair depigmentation, edema, lethargy, liver damage, muscle and fat loss, skin lesions, and weakness (Saeed, 2001; Wang et al., 2005). CySH detection is thus of interest. Moreover, the couple L-cystine/L-cysteine is generally used as a model for the role of the disulfide bond and thiol group in proteins in a variety of biological media (Chen et al., 1999). Therefore, measuring CySH is very important and much effort has been made to develop sensitive methods for its detection. Several methods for thiols and disulfides determination have been reported including chemiluminescence (Rezaei and Mokhtari, 2007; Li et al., 2009; Geoffrey et al., 2011), high-performance liquid chromatography (Yusuke et al., 2009; Peter et al., 2009), fluorimetry (Zhao et al., 2001) and electrochemistry (Liu et al., 2010; Murilo and Iolanda, 2007). Among these, electrochemical analysis has inherent advantages of simplicity, easy miniaturization, high sensitivity, and relatively low cost (Olga et al., 2003, 2004). Therefore, different chemically modified electrodes have been developed for the oxidation and detection of L-cysteine (Chen et al., 2008; Jean et al., 2009; Maleki et al., 2007; Raoof et al., 2005; Razmi and Habibi, 2009). Unfortunately, at ordinary electrodes (Pt, Au, graphite), the electrochemical behaviors of CySH are poor; narrow linear range and high overpotential of electrochemical oxidation are observed (Su and Cheng, 2008; Zhou et al., 2007), even no electrochemical responses could be observed. It has been realized that the method to solve this problem may be to utilize new materials to modify electrodes (Chen et al., 2008). In order to overcome these inherent difficulties, the surface of bare electrodes is being modified with suitable electrocatalysts to improve interfacial electron transfer. Therefore, one material that has been highlighted by presenting a key role in the process of charge transfer is graphene oxide (GO). GO is a single-atom-thick and two-dimensional carbon material that has attracted great attention because of its remarkable electronic, mechanical, and thermal properties (Daniela et al., 2010; Lin et al., 2010; Yang et al., 2010; Zhu et al., 2010a). The synthesis and investigation of the material properties of the stiff materials have been undertaken, although little has been done to explore graphene oxide in the analysis of biomolecules (Dong et al., 2010;

* Corresponding author. Tel.: +86 531 82767161.
E-mail address: ujn.yujh@gmail.com (J. Yu).

0956-5663/$ – see front matter © 2011 Elsevier B.V. All rights reserved.
doi:10.1016/j.bios.2011.09.038

Lu et al., 2009). In addition, different varieties of nanoparticles, such as Pd, Pt (Tang et al., 2010; Zhu et al., 2010b), and quantum dots (Wang et al., 2009), were reported to decorate graphene sheets, which provides a new way to develop catalytic, magnetic, and optoelectronic materials (Bai et al., 2011). GO–Au NCs was prepared via π–π stacking between graphene oxide and Au NCs. Because of the strong quantum confinement of electrons in the ultrasmall size regime, the Au NCs exhibit discrete size-dependent electronic energy level and lose the bulk like electronic properties, Au NCs show "molecule-like" properties (Li et al., 2011; Xie et al., 2009; Wen et al., 2011), such as enhanced catalytic activity, enhanced photoluminescence, and unique charging properties, which render the material promising in various areas ranging from fundamental studies to potential applications, such as catalysis, sensing, to bioimaging. Therefore, GO–Au NCs composite exhibits other fascinating features, including ease of synthesis, good water solubility, low toxicity, surface functionalities, biocompatibility, and excellent stability, which also make them hold great promise in bioanalysis. It is promising to study their properties and applications in electrochemical biosensors.

In the present paper, we demonstrate the ability of water soluble GO as a platform for the sensitive and selective detection of L-cysteine, we report the results of an investigation of the electrochemical oxidation of L-cysteine with GO and Au NCs composite. This composite is a good model for further studies of the determination of other thiols.

2. Materials and methods

2.1. Materials and reagents

Graphite power and L-cysteine were from Sinopharm Chemical Reagent Co. Ltd. (China). Chloroauric acid was purchased from Sigma–Aldrich, Inc. (USA). BSA was from Alfa Aesar China Ltd. Ultrapure water obtained from a Millipore water purification system (18 MΩ, Milli-Q, Millipore, Billerica, MA) was used in all runs. All other reagents were of analytical grade. The 0.1 mol/L phosphate buffer solution (PBS), which was made from Na_2HPO_4, NaH_2PO_4, and H_3PO_4, was employed as a supporting electrolyte.

2.2. Apparatus

The morphologies of GO and GO adsorbed Au NCs were examined with a JEM-2000 transmission electron microscope (TEM) (JEOL Japan). Atomic force microscope (AFM) image was taken by using a SPI3800N microscope (Seiko Instruments Industry Co., Tokyo, Japan) (Seiko Instruments, Inc.) operating in the tapping mode with standard silicon nitride tips. Typically, the surface was scanned at 1 Hz with the resolution of 256 lines/images. The ultraviolet–visible (UV–vis) absorption spectrum of the GO and Au NCs were recorded with a UV-3101 spectrometer (SHIMADAZU, Japan) with 1 cm quartz-cuvette. The FT-IR spectrum was recorded on a Nicolet 400 Fourier transform infrared spectrometer (Madison, WI). Electrochemical measurements were carried out on CHI760D electrochemical workstation (ChenHua Instruments Co., Shanghai, China). A three-electrode system was used in the experiment with a bare and the modified GC electrode (3 mm in diameter) as the working electrode, respectively. An Ag/AgCl electrode (saturated KCl) and a Pt wire electrode were used as reference electrode and counter-electrode, respectively.

2.3. Preparation of graphene oxide

A modified Hummers method was utilized to synthesize the oxidized graphite powders. It was prepared on the basis of a procedure described elsewhere (Daniela et al., 2010) with slight modifications. Typically, 2.0 g of natural graphite, 2.0 g of $NaNO_3$ and 6.0 g of $KMnO_4$ were slowly added to 40 mL of concentrated H_2SO_4 under vigorous stirring at 0 °C. The mixture was then stirred continuously for 1 h below 35 °C to oxidize the graphite. After that, 160 mL of water was added into the mixture and the temperature was increased to higher than 90 °C, and the suspension was maintained at 95 °C for 15 min. The mixture was then poured into 240 mL of ultrapure water, after that 16 mL of H_2O_2 was added into the suspension. After cooling to room temperature, the solid products were filtered, subsequently washed with 5% HCl aqueous solution and water, and dried to obtain graphite oxide. The obtained graphite oxide was dispersed in water to yield a yellow-brown suspension (1 mg/mL). The suspension was ultrasonicated for 10 min using an ultrasonication (300 W), and then centrifuged at 6000 rpm for 5 min to remove the unexfoliated graphite oxide particles to obtain graphene oxide.

2.4. Preparation of BSA-stabilized Au NCs

Au NCs were prepared as reported previously (Xie et al., 2009) with slight modifications. In a typical experiment, aqueous $HAuCl_4$ solution (2 mL, 10 mmol/L, 37 °C) was added to BSA solution (5 mL, 50 mg/mL, 37 °C) under vigorous stirring. NaOH solution (0.5 mL, 1 mol/L) was introduced 2 min later, the mixture was then reduced at once with 3.50 g (92.5 mmol) of $NaBH_4$, forming a dark brown solution and stirred for 30 min, and the reaction was allowed to proceed under vigorous stirring at 37 °C for 12 h. During this period, the color of the colloid gradually changed, from light yellow to light brown, and the red fluorescence emission indicated the nucleation of Au NCs. The as-synthesized Au NCs were purified through continuous ultrafiltration using a 3000 MW filter under centrifugation.

2.5. Preparation of sensor

To prepare the sensor of GO–Au NCs modified glass carbon electrode, GO–Au NCs composites was prepared, which 1 mg/mL GO solution was mixed with 1 mg/mL Au NCs solution with the volume ratio of 1:1 under sonication for 1 h. Prior to modification, the GC electrode was polished with 1, 0.3, and 0.05 μm alumina slurry, rinsed thoroughly with ultrapure water between each polishing step, then washed successively with 1:1 nitric acid, acetone, and ultrapure water in an ultrasonic bath and dried in air. The GO/GC, Au NCs/GC, and GO–Au NCs/GC electrodes were obtained by dropping 20 μL of GO or Au NCs or GO–Au NCs solution on the surface of a well-polished GC electrode and dried in air. Finally, the modified electrodes were activated by several successive scans with a scan rate of 50 mV/s in phosphate buffer solution (pH 7.4) until a steady voltammogram was obtained. The sensor was prepared, the finished sensor was stored at 4 °C when not in use.

2.6. Sample preparation

Human urine samples were prepared according to reference (Chen et al., 2007). Urine was collected in the morning from healthy volunteers (one woman and two men, age range 20–30 years). Free reduced CySH (fCySH) was analyzed immediately after sample collection. For the determination of total CySH (tCySH, including protein-bound, free oxidized, and free reduced CySH), the disulfide bonds were reduced by adding 1.0 mL of a freshly prepared 1.0 mol/L $NaBH_4$ solution (containing 0.05 mol/L NaOH) and 0.06 mL of n-octanol to 2.4 mL of urine. After being mixed, the solution was incubated in a 50 °C water bath for 10 min under gentle stirring. The reduced mixture was then centrifuged at 8000 rpm for 20 min. To the supernatant, an aliquot of 3 mol/L HCl was added in

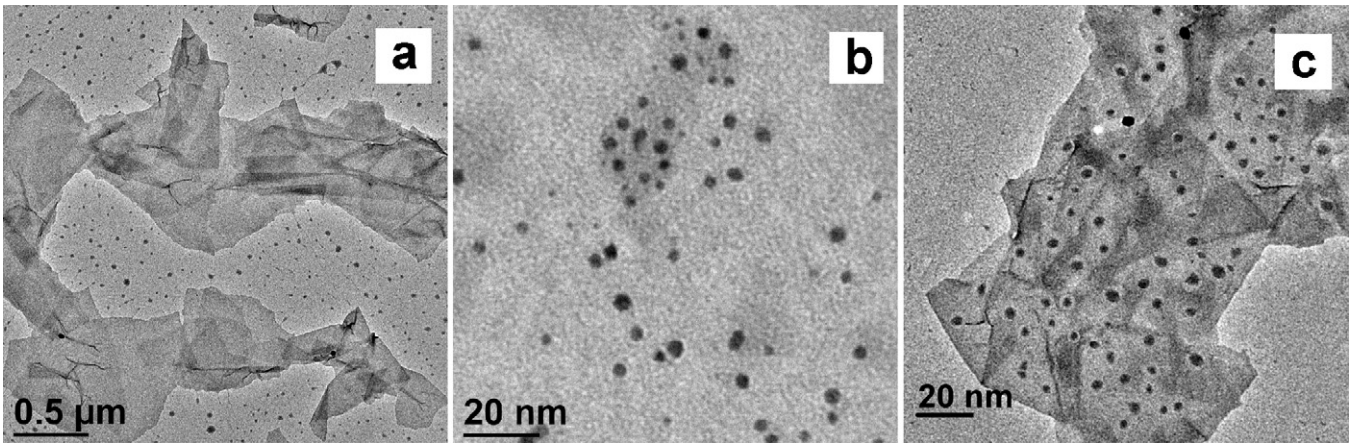

Fig. 1. TEM images of (a) graphene oxide, (b) Au nanocluster, and (c) Au-decorated graphene oxide.

order to decompose excess $NaBH_4$ and adjust the solution pH to ~7.0 (Chwatko and Bald, 2002).

3. Results and discussion

3.1. Characterization of GO–Au NCs composites

Fig. 1a, b and c shows a typical TEM image of graphene oxide, Au nanocluster and GO–Au NCs composites respectively. As can be seen in Fig. 1a, single layer structured GOs with smooth surface are obtained. The TEM image of Au NCs (Fig. 1b) shows a uniform surface topography and the Au NCs have a diameter of about 6.0 nm. After GOs was mixed with Au NCs under sonication for 1 h, there is a homogeneous and dense coverage of Au NCs on the GO surface (Fig. 1c). No aggregation of GO sheets or free Au NCs was observed, which suggests complete deposition of the Au NCs. Moreover, the electrostatic forces were strong enough for the attachment of Au NCs to GO, which was confirmed by the absence of luminescence from the supernatant after centrifugation of the GO–Au NCs composites.

Fig. 2a shows the AFM image of GO in tapping mode. The sample used for AFM observation was prepared by depositing a droplet of GO dispersion (2 μL, 0.01 mg/mL) on a quarts glass sheet and dried under vacuum at room temperature. From the AFM image, the average thickness of GO sheet was confirmed about 1.3 nm, which is in accordance with previous reports (Dong et al., 2010; Daniela et al., 2010). The Au NCs-linked GO array shows brighter spots, particularly at the edges, and also folded structures. The measured height of 7.5 nm corresponds to the theoretical value of an Au NCs (~6 nm) and approximately 45.3% area per spot was linked by Au NCs.

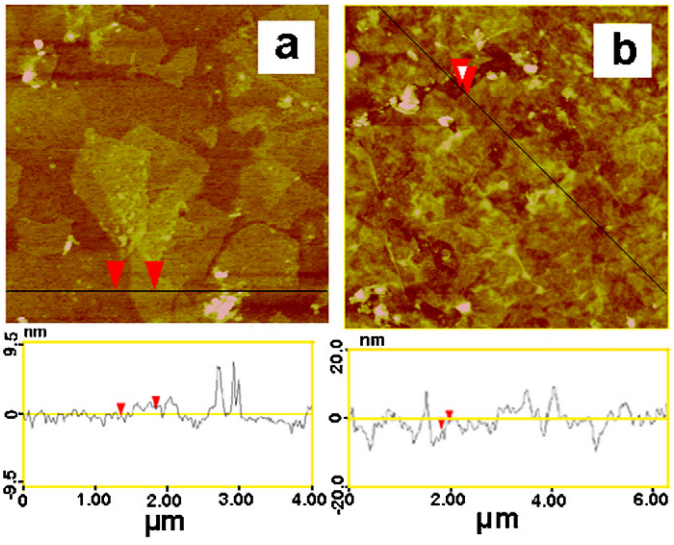

Fig. 2. AFM images (top) and height profile (taken along the black line in the AFM images) of (a) GO sheets and (b) Au NCs–GO composite.

The FT-IR spectra of GO further provided the information of the successful synthesis of GO. As shown in Fig. S1a, the FT-IR spectrum gave the characteristic vibrations of GO, as those reported in previous work (Xu et al., 2008), including a broad and intense peak of O–H group at 3408 cm^{-1}, a C=O peak at 1733 cm^{-1}, an O–H deformation peak at 1401 cm^{-1}, a C–OH stretching peak at 1240 cm^{-1}, a C–O stretching peak at 1061 cm^{-1}, and a peak attributed to the vibrations of unoxidized graphitic skeletal domains and the adsorbed water molecules at 1623 cm^{-1}. Comparing GO, it is clear that the –C–O–C– epoxy groups feature from 1000 to 1200 cm^{-1} becomes a broad band centered at 1035 cm^{-1} (in Fig. S1b), manifesting strong interactions between Au NCs and the epoxy groups.

For comparison, the absorption spectra of Au NCs and GO before and after deposition of the Au NCs were also plotted. The three spectra were recorded for an equal concentration (1 mg/mL) of each material. In the spectrum of GO (Fig. S2a), there are two absorption features: a peak at 227 nm due to the $\pi \rightarrow \pi^*$ transition of C=C, and a shoulder at about 294 nm corresponding to the $n \rightarrow \pi^*$ transition of the C=O bond. However, the adsorption peak of Au NCs (Fig. S2b) in our experiment could still be observed, which suggests a dense coating of Au NCs on the GO sheets. Moreover, no obvious change of the absorption peak of the Au NCs (Fig. S2c) was observed, which indicates that almost no Au NCs agglomerate was formed on the GO sheets, consistent with TEM observations.

3.2. Characterization of the modified electrodes

We firstly investigate the electrochemical behavior of the GO–Au NCs modified electrode using cyclic voltammetry with $K_3Fe(CN)_6$ as the redox probe. Fig. 3 depicts typical cyclic voltammograms of the GO–Au NCs modified electrode in 5 mmol/L $K_3Fe(CN)_6$ and 1 mol/L KCl at different scan rates. One observes that the potentials and peak currents for the $[Fe(CN)_6]^{3-/4-}$ redox processes (anodic and cathodic) show strong dependency upon the scan rates. The peak-to-peak separation becomes slightly widened with increasing scan rate. At the scan rate ranging from 20 to 250 mV/s, both the anodic and the cathodic peak currents increase linearly with the square root of the scan rates (correlation coefficients of 0.9935 and 0.9971 for anodic and cathodic peaks, respectively), suggesting that the reaction is diffusion controlled.

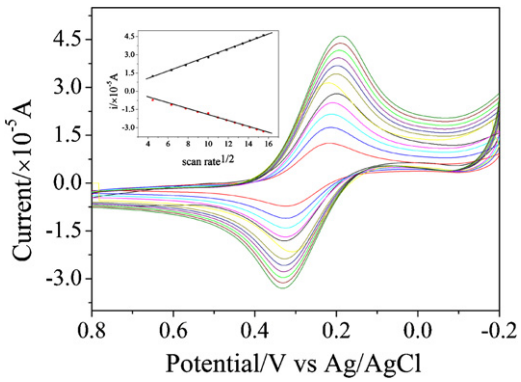

Fig. 3. Cyclic voltammograms of the GO–Au NCs/GC electrode at scan rates from 20 to 250 mV/s in $[Fe(CN)_6]^{3-/4-}$. The inset of panel shows dependence of peak currents on the square root of scan rates GO–Au NCs/GC electrode.

3.3. Cyclic voltammetry of CySH at GO–Au NCs/GC electrode

Fig. S3 shows the electrochemical oxidation of L-CySH at GO/GC (a), Au NCs/GC (b), and GO–Au NCs/GC (c) electrodes at pH 7.4 in PBS buffer solution. Small anodic peaks of L-CySH can be observed at GO/GC electrodes. However, a distinct anodic peak at 0.387 V was observed at the Au NCs/GC electrode and GO–Au NCs/GC. This means both GO and Au NCs clearly plays an important role in the oxidation of L-CySH at pH 7.40. The peak may originate from protonation/depronation of the oxygen-containing functional groups of GO. These are attributed to the high edge-plane-like defective sites existing on GO, which provide many active sites for electron transfer to biological species, contribute to the enhanced activity of carbon materials towards oxidation/reduction of biomolecules (Banks and Compton, 2005; Banks et al., 2005; Zhou et al., 2009). In addition, Au NCs has high specific surface, good catalytic performance to the L-CySH. So, GO–Au NCs/GC electrode has stronger catalytic performance than others.

3.4. Optimization of conditions for electrochemical detection

We investigated the electrochemical current response of modified electrode to pH values in PBS. It was found that the modified electrode themselves gave a peak ratio increment with a change in the pH value from 2.0 to 10.0. The optimum electrochemical current was obtained in the range of pH values from 6.0 to 9.0. Considering that L-cysteine remains active at pH 5.0–7.6, pH 7.4 was selected in this study. According to the other reported electrodes (Nicolae et al., 2001), we conceive the oxidation of GSH at the GO–Au NCs/GC electrode undergoes two processes at pH 7.4. However, the peak potentials are shifted towards the negative potentials because GO–Au NCs enhances the rate of electron transfer. The mechanism proposed is as follows:

$$CySH \leftrightarrow CyS^- + H^+ \quad (1)$$

$$CyS^- \rightarrow CyS + e^- \quad (2)$$

$$2CyS \rightarrow CySSyC \quad (3)$$

The effect of the concentration of GO and Au NCs in the GO–Au NCs composite on the response of the sensor towards L-cysteine was investigated. With the increasing of the GO concentration from 0 to 2.0 mg/mL, the current response of the electrode to 5.0 μmol/L L-cysteine was increased gradually, and reached the maximum at 1.0 mg/mL GO. The increase of sensitivity result from that the increase of GO concentration improved the electroactivity. Further increase the GO concentration from 1.0 to 2.0 mg/mL resulted in the decrease of the sensitivity of the sensor. This might be the reason that excessive GO may be stacked each other with further increase of GO in the modifying layer. This process will entrap Au NCs between the GO layers which lead to the decrease peak current. So 1.0 mg/mL of GO concentration was selected as optimal condition to prepare the sensor. Similar results were obtained for the concentration of Au NCs and also a 1.0 mg/mL of Au NCs concentration was selected.

3.5. Reproducibility, stability, and selectivity of sensor

The reproducibility of the assay system was evaluated by intra- and inter-assay coefficients of variation. The intra-assay precision of the sensor was evaluated by assaying L-cysteine at two levels for five replicative measurements. The intra-assay variation coefficients with this method were 3.1% and 5.8% at L-cysteine concentrations of 2.0 and 8.0 μmol/L, respectively, showing a good repeatability. While the inter-assay variation coefficients at these concentrations on five sensors made independently were 4.9% and 3.7%, respectively, indicating acceptable fabrication reproducibility. When the sensor was not in use, it was stored at 4 °C. 94.7% of the initial response of the sensor for L-cysteine remained after 4 weeks, and 87.3% of the initial response remained after 12 weeks. These results indicated the sensor had acceptable stability.

To demonstrate the selectivity for detecting L-cysteine, for L-cysteine determinations in biological samples, the main interference may come from glutathione and cystine, which always coexists with L-cysteine. 10 μmol/L glutathione and 10 μmol/L cystine did not affect the detection of 0.2 μmol/L L-cysteine under the optimum conditions. If the coexisting compounds caused a relative error of less than ±5%, they were considered to have no interference with the detection of L-cysteine. The results revealed that the proposed method might be applied to the detection of L-cysteine in the biological samples. The effect of the following substances on the determination of L-cysteine was investigated: Mg^{2+}, Ca^{2+}, Fe^{3+}, Al^{3+}, Zn^{2+}, Mn^{2+}, sucrose, glucose, lactose, urea, uric acid, thymine, guanine, adenine, L-Met, L-Asp, L-Ala, L-Pro, L-Glu, L-His, L-Phe, L-Arg, L-Gly, L-Lys, L-Trp. The ratios of these coexisting substances to the concentration of L-cysteine (0.2 μmol/L) were fixed at 100. It was found that these ions, carbohydrates and nucleotide acids had no distinct effect on the determination of L-cysteine. Amino acids had almost no interference on the detection of L-cysteine. This high selectivity maybe ascribe to the low oxidation potential for L-cysteine which can minimize the response of interfering substances.

3.6. Analytical performance characteristics

The sharp and well-defined peak current (Fig. 4a) increased with L-cysteine concentration. A calibration curve between the anodic peak current at 0.387 V and the L-cysteine concentration was exhibited in Fig. 4b. As can be seen, at the high concentration range, the anodic peak currents tend to be stable, indicating that the GO–Au NCs were almost interacted by L-cysteine molecules. A linear relationship between the anodic peak current and L-cysteine concentration was obtained covering the concentration range from 0.05 to 20.0 μmol/L; the linear regression equation is I (μA) = −3.08 − 6.41c (μmol/L), with a correlation coefficient of 0.9949. The detection limit is calculated to be 0.02 μmol/L based on the 3σ of the blank signals. The characteristics of partial sensors for L-cysteine are summarized in Table 1. Compared with the other sensors, the proposed sensor features a lower detection limit and lower oxidative potential, they are all related to the same reference electrode Ag/AgCl (saturated KCl).

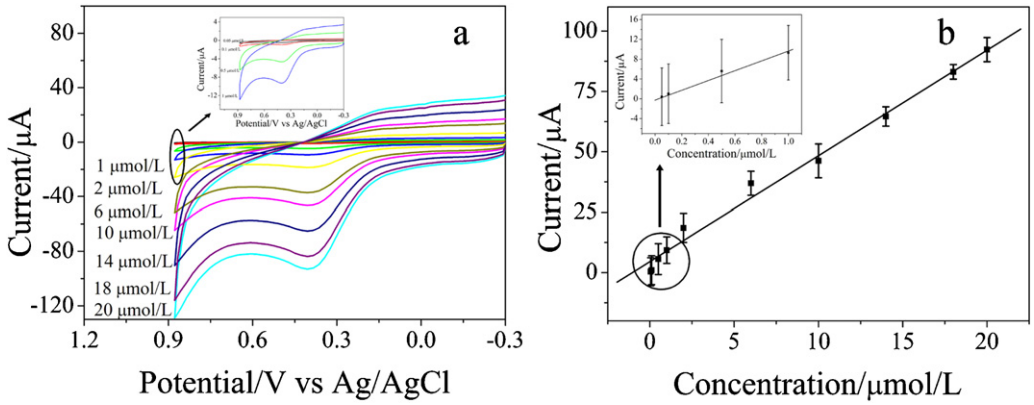

Fig. 4. CV grams (a) at GO–AuNCs modified electrode in solutions containing 1.0, 2.0, 6.0, 10.0, 14.0, 18.0 and 20.0 μmol/L L-cysteine. The calibration curve (b) corresponding to amperometric responses. Scan rate: 50 mV/s. Error bar = ±standard deviation.

Table 1
Comparison of major characteristics of some modified electrodes used in the electrocatalysis of L-cysteine.

Electrode	Dynamic range/μmol/L	Detection limit/μmol/L	Oxidation potential/V /vs. Ag/AgCl (saturated KCl)	References
Nafion/PbNP modified carbon ceramic electrode	1–67.2	0.46	+0.78	Razmi and Habibi (2009)
Glassy carbon electrode modified with poly (5-amino-2-mercapto-1,3,4-thiadiazole)	20–180	3.36	+0.55	Palraj and John (2009)
Pt nanoparticles/poly(o-aminophenol) film on glassy carbon electrode	0.4–6.3	0.08	+0.42	Liu et al. (2010)
Pristine GaN nanowires electrode	0.5–75	0.042	–	Lai et al. (2010)
Ordered mesoporous carbon-modified glassy carbon electrode	18–2500	0.05	+0.35	Zhou et al. (2007)
BB FCF-modified Nafion-coated electrode	10–100	0.5	+0.9	Chen et al. (2008)
Tin pentacyanonitrosylferrate-modified carbon ceramic electrode	1–51	0.62	+0.9	Razmi and Heidari (2009)

Table 2
Determination of CySH in urine samples using the GO–Au NCs/GC electrode ($n = 5$).

Samples	f-CySH measured/ μmol/L	R.S.D./%	Spiked/ μmol/L	Recovery/%	Chemiluminescence/ μmol/L	t-CySH measured/ μmol/L	R.S.D./%	Spiked/ μmol/L	Recovery/%	Chemiluminescence/ μmol/L
			5.00	93.18				10.00	103.80	
1	12.95 ± 0.51	3.95	10.00	103.59	12.17 ± 1.10	88.01 ± 4.51	5.13	20.00	94.10	93.14 ± 2.15
			15.00	97.21				30.00	103.67	
			5.00	102.81				10.00	94.37	
2	10.39 ± 0.54	5.17	10.00	96.13	11.62 ± 0.69	75.29 ± 3.65	4.85	20.00	106.42	77.38 ± 4.17
			15.00	106.29				30.00	103.85	
			5.00	95.20				10.00	98.19	
3	14.19 ± 0.41	2.86	10.00	97.17	14.95 ± 0.71	95.13 ± 3.20	3.36	20.00	104.37	91.04 ± 5.06
			15.00	104.80				30.00	106.25	

Mean value ± S.D.

3.7. Detection of CySH in real samples

To confirm the feasibility, the proposed method had been applied to determine L-cysteine in human urine. The levels of both free reduced and total CySH in three human urine samples were tested by using the GO–Au NCs modified electrode, and the results obtained are shown in Table 2. Each recovery of L-cysteine was determined by comparing the results obtained before and after the addition of standard L-cysteine to the diluted uric samples. Note that the detection sensitivity was generally lower in the presence of urine samples, which might be ascribed to the matrix effect. To confirm the validity of the results, different amounts of CySH at levels similar to those found in the samples were spiked; the recoveries obtained were reasonably good, varying between 93.18 and 106.29% with a satisfying analytical precision (R.S.D. ≤ 5.17%), which validated the reliability and practicality of this method.

Table 2 showed the results obtained from analysis of different samples by using the introduced work and a chemiluminescence method (Geoffrey et al., 2011) as a reference method in order to statistically verify the performance of the sensor for CySH determination. The results obtained showed that CySH contents, as measured by the proposed method were in excellent agreement with those obtained by chemiluminescence method. The *t*-test showed there was no significant difference between this method and chemiluminescence method at a confidence level of 95%.

4. Conclusion

In this work, an electrochemical biosensor based on GO–Au NCs composites for L-cysteine was fabricated. The electrochemical investigation demonstrate that GO–Au NCs composite can provide a suitable catalytic platform for L-cysteine, which greatly facilitated the electron-exchange between L-cysteine and electrode, increased the sensitivity and decreased the overpotentials for the oxidation of L-cysteine. The as-prepared GO–Au NCs composite layer

demonstrated excellent conductivity, extraordinary electron transport properties, and large specific surface area, which resulted in high electrochemical current response and made it a promising candidate for development of an electrochemical sensor. Further experiments are in progress in order to improve the detection limit and to extend the method to other thiols and disulfides compounds.

Acknowledgments

This work was financially supported by Natural Science Research Foundation of China (21175058; 51003039), Natural Science Foundation of Shandong Province, China (ZR2011BQ019), Excellent Young and Middle-Aged Scientist Reward Foundation of Shandong Province (Grant No. 2008BS09006) and Technology Development Plan of Shandong Province, China (Grant Nos. 2011GGB01153; 2009GG20003022).

Appendix A. Supplementary data

Supplementary data associated with this article can be found, in the online version, at doi:10.1016/j.bios.2011.09.038.

References

Ardakani, M.M., Rahimi, P., Karami, P.E., Hamid, R.Z., Naeimi, H., 2007. Sens. Actuators B 123, 763–768.
Bai, H., Li, C., Shi, G.Q., 2011. Adv. Mater. 23, 1089–1115.
Banks, C.E., Compton, R.G., 2005. Analyst 130, 1232–1239.
Banks, C.E., Davies, T.J., Wildgoose, G.G., Compton, R.G., 2005. Chem. Commun. 829, 829–841.
Chen, H.L., Li, M.S., 1999. Structure and Function of Biomacromolecules. Shanghai Science Press, Shanghai.
Chen, S.M., Chen, J.Y., Thangamuthu, R., 2008. Electroanalytical 20, 1565–1573.
Chen, Z.F., Zheng, H.Z., Lu, C., Zu, Y.B., 2007. Langmuir 23, 10816–10822.
Chwatko, G., Bald, E., 2002. J. Chromatogr. A 949, 141–151.
Daniela, C.M., Dmitry, V.K., Jacob, M.B., Alexander, S., Sun, Z.Z., Alexander, S., Lawrence, B.A., Lu, W., James, M.T., 2010. ACS NANO 4, 4806–4814.
Dong, H.F., Gao, W.C., Yan, F., Ji, H.X., Ju, H.X., 2010. Anal. Chem. 82, 5511–5517.
Geoffrey, P.M., Jessica, M.T., Xavier, A.C., Neil, W.B., Paul, S.F., 2011. Anal. Chem. 83, 6034–6039.
Jean, C.N., Bai, J., Qi, B., Guo, L.P., 2009. Anal. Biochem. 386, 79–84.
Lai, Y.T., Ganguly, A., Chen, L.C., Chen, K.H., 2010. Biosens. Bioelectron. 26, 1688–1691.
Li, L.L., Liu, H.Y., Shen, Y.Y., Zhang, J.R., Zhu, J.J., 2011. Anal. Chem. 83, 661–665.
Li, S.F., Zhang, X.M., Du, W.X., Ni, Y.H., Wei, X.W., 2009. J. Phys. Chem. C 113, 1046–1051.
Lin, Y., Zhang, K., Chen, W.F., Liu, Y.D., Geng, Z.G., Zeng, J., Pan, N., Yan, L.F., Wang, X.P., Hou, J.G., 2010. ACS NANO 4, 3033–3038.
Liu, L.P., Yin, Z.J., Yang, Z.S., 2010. Bioelectrochemistry 79, 84–89.
Lu, C.H., Yang, H.H., Zhu, C.L., Chen, X., Chen, G.N., 2009. Angew. Chem. Int. Ed. 48, 4785–4787.
Maleki, N., Safavi, A., Sedaghati, F., Tajabadi, F., 2007. Anal. Biochem. 369, 149–153.
Murilo, S., Iolanda, C.V., 2007. Sens. Actuators B 128, 279–285.
Nicolae, S., Bulusu, V.S., Elena, P., Donald, A.T., Akira, F., 2001. Anal. Chem. 73, 514–519.
Olga, N., Nathan, S.L., Richard, G.C., 2003. Talanta 60, 1085–1095.
Olga, N., Nathan, S.L., Richard, G.C., 2004. Electroanalytical 16, 1285–1291.
Palraj, K., John, S.A., 2009. Electrochem. Commun. 11, 367–370.
Peter, M., Gyula, W., Eszter, K., Sandor, T., 2009. J. Chromatogr. B 877, 3331–3346.
Raoof, J.B., Ojani, R., Kolbadinezhad, M., 2005. Electroanalytical 17, 2043–2051.
Razmi, H., Habibi, E., 2009. Electroanalytical 21, 867–874.
Razmi, H., Heidari, H., 2009. Anal. Biochem. 388, 15–22.
Rezaei, B., Mokhtari, A., 2007. Spectrochim. Acta A 66, 359–363.
Saeed, S., 2001. Anal. Chem. 73, 5972–5978.
Su, W.Y., Cheng, S.H., 2008. Electrochem. Commun. 10, 899–902.
Tang, Z.H., Shen, S.L., Zhuang, J., Wang, X., 2010. Angew. Chem. Int. Ed. 49, 4603–4607.
Wang, W.H., Rusin, O., Xu, X.Y., Kyu, K.K., Jorge, O.E., Sayo, O.F., Kristin, A.F., Mark, L., Corin, M.S., Candace, M.L., Frank, R.F., Isiah, M.W., Robert, M.S., 2005. J. Am. Chem. Soc. 127, 15949–15958.
Wang, Y., Lu, J., Tang, L.H., Chang, H.X., Li, J.H., 2009. Anal. Chem. 81, 9710–9715.
Wen, F., Dong, Y.H., Feng, L., Wang, S., Zhang, S.C., Zhang, X.R., 2011. Anal. Chem. 83, 1193–1196.
Xie, J.P., Zheng, Y.G., Jackie, Y.Y., 2009. J. Am. Chem. Soc. 131, 888–889.
Xu, Y.X., Bai, H., Lu, G.W., Li, C., Shi, G.Q., 2008. J. Am. Chem. Soc. 130, 5856–5857.
Yang, W.R., Kyle, R.R., Simon, P.R., Pall, T., Gooding, J.J., Filip, B., 2010. Angew. Chem. Int. Ed. 49, 2114–2138.
Yusuke, I., Yusuke, S., Yuki, N., Keisuke, M., Osamu, S., Rie, I., Koichi, S., Hiroyuki, N., 2009. J. Chromatogr. B 877, 3309–3317.
Zhao, C., Zhang, J., Song, J., 2001. Anal. Biochem. 297, 170–176.
Zhou, M., Ding, J., Guo, L.P., Shang, Q.K., 2007. Anal. Chem. 79, 5328–5335.
Zhou, M., Zhai, Y.M., Dong, S.J., 2009. Anal. Chem. 81, 5603–5613.
Zhu, Y.W., Shanthi, M., Cai, W.W., Li, X.S., Ji, W.S., Jeffrey, R.P., Rodney, S.R., 2010a. Adv. Mater. 22, 3906–3924.
Zhu, C.Z., Guo, S.J., Zhai, Y.M., Dong, S.J., 2010b. Langmuir 26, 7614–7618.